Journal of Ceramic Processing Research. Vol. 17, No. 6, pp. 615~619 (2016)

J O U R N A L O F
Ceramic Processing Research

The role of La content on microstructure and magnetic characteristics of the $Sr_{1-x}La_xFe_{11.80}Cu_{0.20}O_{19}$ hexagonal ferrites

Yujie Yang*, Fanhou Wang, Juxiang Shao and Qilong Cao
Computational Physics Key Laboratory of Sichuan Province, Yibin University, Yibin 644007, P. R. China

Hexagonal ferrites $Sr_{1-x}La_xFe_{11.80}Cu_{0.20}O_{19}$ magnetic powders and magnets were prepared by the solid state reaction. The phase compositions of the magnetic powders were identified by X-ray diffraction. There is a single magnetoplumbite phase in the magnetic powders with x from 0.12 to 0.32, and for the magnetic powders with $x \geq 0.36$, the $LaFeO_3$ phase is observed. The microstructures of the magnets were investigated by a field emission scanning electron microscopy. The magnets are formed of hexagonal-shaped crystals and the particles are distributed homogeneously. The magnetic properties of the magnets were measured by a magnetic properties test instrument. The remanence of the magnets increases with x from 0.12 to 0.40. However, the intrinsic coercivity, magnetic induction coercivity and maximum energy product of the magnets first increase with x from 0.12 to 0.24, and then begin to decrease when x continues to increase.

Key words: M-type hexaferrites, La content, La-Cu substitution, Magnetic properties.

Introduction

The hexagonal ferrites (Ba, Sr)$Fe_{12}O_{19}$ have been widely used in applications such as permanent magnets, microwave devices, magneto-optics and magnetic recording media due to their low cost, excellent chemical stability and corrosion resistance [1, 2]. In order to obtain magnetic materials with the appropriate remanence and coercivity, adding or doping some elements were widely used. Several studies on hexagonal ferrites of substitution of Sr ions with different cations, such as La^{3+}, Pr^{3+}, Nd^{3+} and Sm^{3+} [3-6]. Several studies on hexagonal ferrites in which Fe ions are substituted by different cations have been carried out to obtain the hexagonal ferrites with appropriate magnetic properties. Among the investigated substitutions are Co^{2+}, Cr^{3+}, Ti^{4+}, Al^{3+} and Sn^{4+} [7-11]. The hexagonal ferrites with combined substitution such as La-Co, La-Zn, La-Cu, Co-Ti and La-CoZn have been reported [12-17].

Although Qiao et al. [14] and Yang et al. [15] have reported the influence of La-Cu substitution on magnetic properties of strontium hexaferrites, the effects of La content on the microstructure and magnetic characteristics of La-Cu substituted strontium hexaferrites have been rarely investigated. In the present paper, the hexaferrite $Sr_{1-x}La_xFe_{11.80}Cu_{0.20}O_{19}$ magnetic powders and magnets were synthesized by the solid state reaction. The role of La content (x) on the microstructure and magnetic characteristics of the $Sr_{1-x}La_xFe_{11.80}Cu_{0.20}O_{19}$ hexagonal ferrites has been studied systematically.

*Corresponding author:
Tel : +86 831 3531171
Fax: +86 831 3531161
E-mail: loyalty-yyj@163.com

Experimental Procedure

The hexaferrite $Sr_{1-x}La_xFe_{11.80}Cu_{0.20}O_{19}$ magnetic powders and magnets were prepared according to the solid state reaction. The starting materials used in this study were $SrCO_3$ (99% purity), La_2O_3 (99% purity), Fe_2O_3 (99% purity) and CuO (99% purity), mixed together in the nominal composition of $Sr_{1-x}La_xFe_{11.80}Cu_{0.20}O_{19}$, where the La content (x) varies from 0.12 to 0.40 with about 0.04 increment. Mixtures of the starting materials were milled in water for 8 hours with an angular velocity of 80 rpm and a ball-to-power weight ratio of 12 : 1. The milling processes were performed in a ball mill using hardened steel balls (diameter 8 mm). The mixed power was dried, crushed, and sifted. The sifted powders were made into balls (diameter about 8 mm), and the temperature was increased up to 1250 °C in a laboratory furnace; and then these balls were calcined for 2 hours in air atmsosphere. The calcined balls were shattered to particles less than 100 μm using a vibration mill, then wet-milled with additives ($CaCO_3$, SiO_2, Al_2O_3 and H_3BO_3) for 14 hours using a ball-mill. The finely milled slurry with a diameter of about 0.75 μm was pressed into disc-shaped pellets (diameter 8 mm, thickness 15 mm) under 310 MPa in the magnetic field of 900 kA/m, which was parallel to the pressing direction. The green pellets were sintered in a laboratory furnace at 1180 °C for 1.5 hours in air atmosphere.

The phase compositions of the magnetic powders were determined using a PANalytical X'Pert Pro diffractometer in continuous mode with Cu K_α (λ = 1.5406 Å) radiation. The micrographs of the magnets were observed using a HITACHI S-4800 field emission scanning electron microscopy (FESEM). The magnetic properties of the magnets were measured at room temperature using a magnetic properties test instrument (Model MATS-2000, National Institute of Metrology of China).

Results and Discussions

Fig. 1 shows the XRD patterns of the hexaferrite $Sr_{1-x}La_xFe_{11.80}Cu_{0.20}O_{19}$ magnetic powders with different La content (x) varied from 0.12 to 0.40. It can be seen that for the magnetic powders with x from 0.12 to 0.32, all the X-ray diffraction peaks are corresponding to a single phase magnetoplumbite structure of strontium hexaferrite. For the magnetic powders with $x \geq 0.36$, the $LaFeO_3$ phase is observed. For the magnetic powders with x from 0.12 to 0.24, the strongest peak is (008). For the magnetic powder with x of 0.32, the strongest peak is (107). For the magnetic powders with x of 0.28, 0.36 and 0.40, the strongest peak is (114). This indicates that La content (x) plays an important role in the formation of the single-phase hexaferrite.

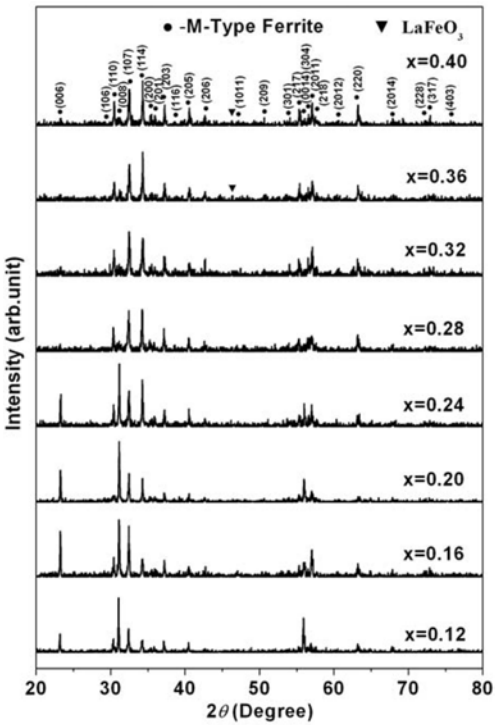

Fig. 1. XRD patterns of the hexaferrite $Sr_{1-x}La_xFe_{11.80}Cu_{0.20}O_{19}$ magnetic powders with different La content (x).

Table 1. Lattice contants c and a, ratio of c/a for the hexaferrite $Sr_{1-x}La_xFe_{11.80}Cu_{0.20}O_{19}$ magnetic powders with different La content (x).

La content (x)	c (Å)	a (Å)	c/a
0.12	23.0089	5.8935	3.9041
0.16	23.0001	5.8953	3.9014
0. 20	22.9897	5.8948	3.9000
0.24	22.9782	5.8927	3.8994
0.28	22.9686	5.8964	3.8954
0.32	23.9592	5.8922	3.8965
0.36	22.9495	5.8943	3.8935
0.40	22.9424	5.8941	3.8924

The lattice paramenters c and a are calculated from the values of d_{hkl} corresponding to (008) peaks and (107) peaks according to the equation given by [18]:

$$d_{hkl}=\left(\frac{4}{3}\cdot\frac{h^2+hk+k^2}{a^2}+\frac{l^2}{c^2}\right)^{-1/2} \quad (1)$$

where d_{hkl} is the crystal face distance and values h, k and l are the Miller indices. The lattice paramenters c and a, ratio of c/a for the hexaferrite $Sr_{1-x}La_xFe_{11.80}Cu_{0.20}O_{19}$ magnetic powders with different La content (x) are listed in Table 1. It is evident that the lattice parameter c decreases with increasing x from 0.12 to 0.40. However, compared with the lattice parameter c, the lattice parameter a is more or less constant. The decrease of the lattice parameter c can be due to the smaller ionic radius of La^{3+} (1.22 Å) compared to Sr^{2+} (1.32 Å), which decreases the distance between stacking layers in c-direction.

Fig. 2 shows the representative FE-SEM images of the hexaferrite $Sr_{1-x}La_xFe_{11.80}Cu_{0.20}O_{19}$ magnets with La content (x) of 0.12, 0.24, 0.32 and 0.40. It can be seen from the figure that the magnets have formed the hexagonal structures and the particles are distributed evenly. In addition, the mean particle size of the magnets is basically not changed with the increase of x.

The influence of La content (x) on the remanence (B_r) of the hexaferrite $Sr_{1-x}La_xFe_{11.80}Cu_{0.20}O_{19}$ magnets is shown in Fig. 3. It is observed that B_r of the magnets increases from 409.5 to 426.2 mT with x increased from 0.12 to 0.40. The increase of B_r can be attributed to increase in hyperfine fields at 12k and 2b sublattice sites or increase in the Fe^{3+}-O-Fe^{3+} superexchange

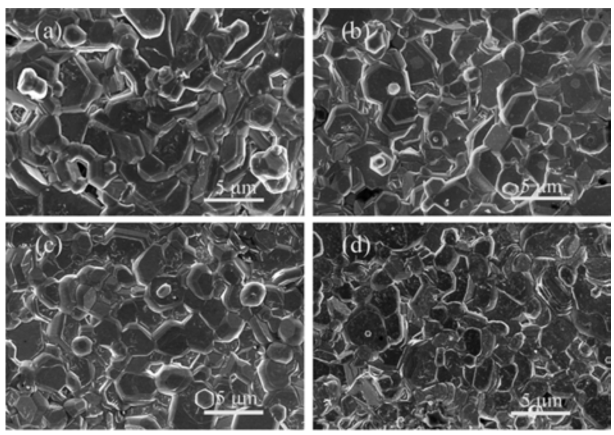

Fig. 2. FE-SEM micrographs of the hexaferrite $Sr_{1-x}La_xFe_{11.80}Cu_{0.20}O_{19}$ magnets; (a) x = 0.12, (b) x = 0.24, (c) x = 0.32 and (d) x = 0.40.

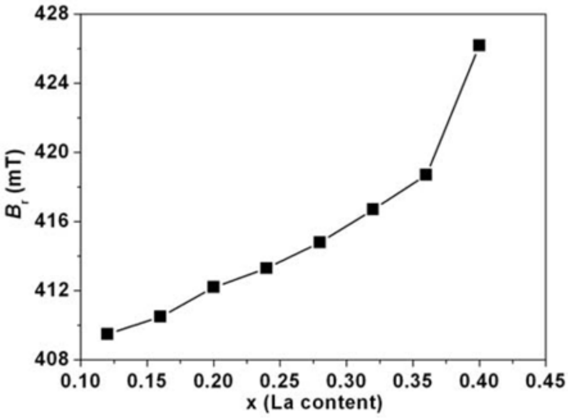

Fig. 3. The remanence (B_r) of the hexaferrite $Sr_{1-x}La_xFe_{11.80}Cu_{0.20}O_{19}$ magnets as a function of La content (x).

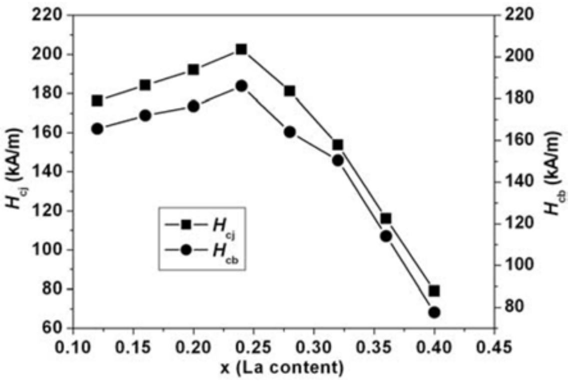

Fig. 4. The intrinsic coercivity (H_{cj}) and magnetic induction coercivity (H_{cb}) of the hexaferrite $Sr_{1-x}La_xFe_{11.80}Cu_{0.20}O_{19}$ magnets as a function of La content (x).

interaction at 2b and 12k sites, as reported in previous works [3, 19]. When the La content (x) is increased from 0.12 to 0.40, the lattice parameter *c* decreases as shown in Table 1. And then, the Fe^{3+}-O^{2-} distance that is parallel to the c-axis decreases, which will cause the Fe^{3+}-O-Fe^{3+} superexchange interaction strength to increase. This results in an increase in the hyperfine fields at 2b and 12k sites.

Fig. 4 shows the influence of La content (x) on the intrinsic coercivity (H_{cj}) and magnetic induction coercivity (H_{cb}) of the hexaferrite $Sr_{1-x}La_xFe_{11.80}Cu_{0.20}O_{19}$ magnets. As seen from the figure, H_{cj} and H_{cb} of the magnets first increases from 176.2 and 165.6 kA/m (at x = 0.12) to 202.5 and 186.0 kA/m (at x = 0.24), respectively. With a further increase in the La content (x), H_{cj} and H_{cb} decreases drastically, and reach to 78.9 and 77.6 kA/m at x = 0.40. The change of the coercivity with La content is in agreement with that reported by Liu et al.[3] and Wang et al. [20]. The coercivity of the magnets depends both on their magnetocrystalline anisotropy and on their microstructure. According to the literature [21], the coercivity can be described by the following expression:

$$H_c = aH_a - \frac{N(B_r + J_s^0)}{\mu_0} \quad (2)$$

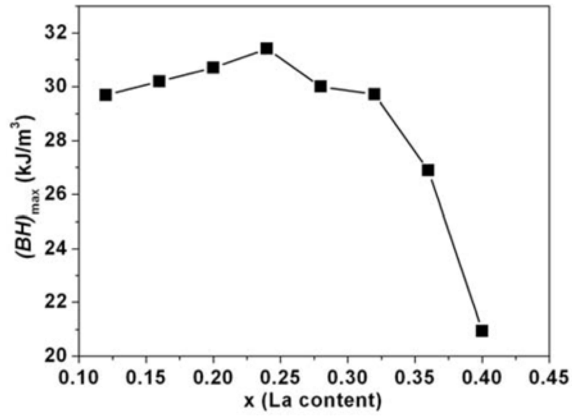

Fig. 5. The maximum energy product [$(BH)_{max}$] of the hexaferrite $Sr_{1-x}La_xFe_{11.80}Cu_{0.20}O_{19}$ magnets as a function of La content (x).

where α is the microstructure factor, *N* is the grain demagnetization factor, H_a is the magnetocrystalline anisotropy field, and J_s^0 is the saturation polarization of the magnet. The factor *α* increases with decreasing grain size, thus reflecting the well-known H_c-grain size depency; the factor *N* is govern by the grain shape and increases when the grain shape becomes more platelet shaped. The representative FESEM micrographs shown in Fig. 2 exhibit that the mean particle size and particle morphology of the magnets do not change basically with the increase of x, which implies that the factors *á* and *N* remain constant. Therefore, it can be concluded that the increase of H_{cj} and H_{cb} with increasing x from 0.12 to 0.24 can be due to the magnetocrystalline anisotropy field increase with increasing La content. As the content of La^{3+} increases, the Fe^{3+} ions present at octahedral sites are forced to migrate towards the tetrahedral sites. It leads to the conversion of Fe^{3+} (high spin) into Fe^{2+} (low spin) to maintain the electrical neutrality of M-type hexaferrite. The formation of any low spin iron ions on thetetrahedral site during processing, preferentially occupy 2a octahedral site [22]. As a result, the number of Fe^{2+} ions on octahedral site increases with increasing La content. The Fe^{2+} ions enhance the coercivity due to strong magnetocrystalline anisotropy of Fe^{2+} on 2a sites [22, 23]. And this leads to an increase in coercivity. On the other hand, the decrease of H_{cj} and H_{cb} with increasing x from 0.24 to 0.40 can be attributed to two factors. The first factor is that an increase in the abundance of Fe^{2+} ions, which arises with increasing x, will destroy the regular atomic arrangement of the Fe^{3+} ions, and this results in a decrease in coercivity [24]. The second one is that the amount of magnetic impurities such as the $LaFeO_3$ phase which will destroy the regular atomic arrangement of the Fe^{3+} ions increases with the increase of x shown in Fig. 1, which leads to a reduction in coercivity [20].

The influence of La content (x) on the maximum energy product [$(BH)_{max}$] of the hexaferrite Sr_{1-x}

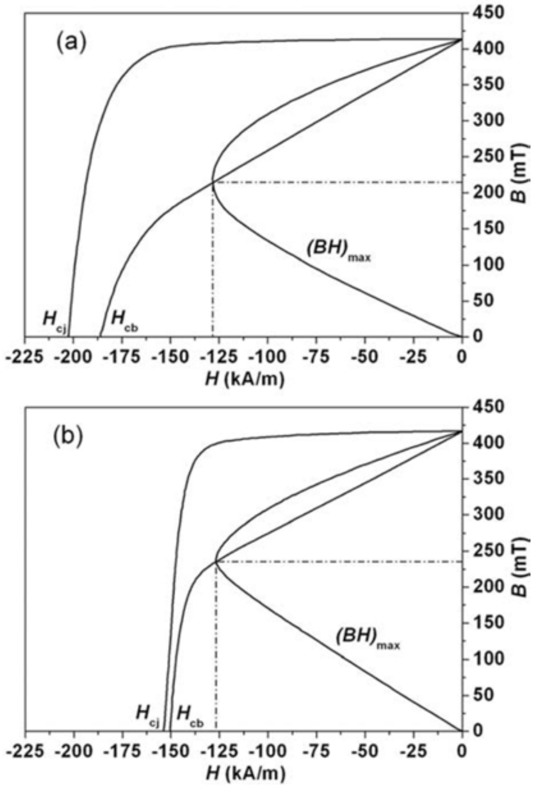

Fig. 6. Typical demagnetizing curves for the hexaferrite $Sr_{1-x}La_xFe_{11.80}Cu_{0.20}O_{19}$ magnets measured at room temperature; (a) x = 0.24 and (b) x = 0.32.

$La_xFe_{11.80}Cu_{0.20}O_{19}$ magnets is shown in Fig. 5. It is evident that $(BH)_{max}$ initially increases with x from 0.12 to 0.24, and then begins to decrease when x continues to increase. At x = 0.24, $(BH)_{max}$ reaches to the maximum value of 31.41 kJ/m^3. The larger the maximum energy product is, the better the magnet is. Since the maximum energy product $[(BH)_{max}]$ is the maximum area in second quadrant of the hysteresis loop, the values of remanence (B_r) and magnetic induction coercivity (H_{cb}) will have their influence on it. From Fig. 4 and Fig. 5, the change of $(BH)_{max}$ has the same feature as that of H_{cb} as shown in Fig. 4.

Fig. 6 presents two typical demagnetizing curves for the hexaferrite $Sr_{1-x}La_xFe_{11.80}Cu_{0.20}O_{19}$ magnets measured at room temperature with La content (x) of 0.24 and 0.32. As seen from Fig. 6(a), the magnet with x of 0.24 exhibits the magnetic properties, including the remanence (B_r = 413.3 mT), intrinsic coercivity (H_{cj} = 202.5 kA/m), magnetic induction coercivity (H_{cb} = 186.0 kA/m) and maximum energy product $[(BH)_{max}$ = 31.41 kJ/m$^3]$. As seen from Fig. 6(b), the magnet with x of 0.32 shows the magnetic properties, including the remanence (B_r = 416.7 mT), intrinsic coercivity (H_{cj} = 153.8 kA/m), magnetic induction coercivity (H_{cb} = 150.5 kA/m) and maximum energy product $[(BH)_{max}$ = 29.71 kJ/m$^3]$.

Conclusions

Hexagonal ferrite $Sr_{1-x}La_xFe_{11.80}Cu_{0.20}O_{19}$ magnetic powders and magnets were synthesized according to the solid state reaction. X-ray diffraction was used to identify the phase compositions of the magnetic powders. There is a single magnetoplumbite phase in the magnetic powders with x from 0.12 to 0.32, and for the magnetic powders with x ≥ 0.36, the $LaFeO_3$ phase is observed. A field emission scanning electron microscopy was employed to investigate the microstructures of the magnets. The magnets are formed of hexagonal-shaped crystals and the particles are distributed evenly.

The magnetic properties of the magnets were measured by a magnetic properties test instrument. B_r of the magnets increases from 409.5 mT (at x = 0.12) to 426.2 mT (at x = 0.40). However, H_{cj} and H_{cb} of the magnets first increase from 176.2 and 165.6 kA/m (at x = 0.12) to 202.5 and 186.0 kA/m (at x = 0.24), respectively. With a further increase in the La content, H_{cj} and H_{cb} decrease drastically. $(BH)_{max}$ of the magnets first increases with x from 0.12 to 0.24, and then begins to decrease when x continues to increase.

References

1. C.J. Li, J.N. Wang, Mater. Lett. 64 (2010) 207-214.
2. M.J. Iqbal, S. Faroop, J. Alloys Compd. 493 (2010) 595-600.
3. X. Liu, W. Zhong, S. Yang, Z. Yu, B. Gu, Y. Du, J. Magn. Magn. Mater. 238 (2002) 207-214.
4. J.F. Wang, C.B. Ponton, I.R. Harris, J. Alloys Compd. 403 (2005) 104-109.
5. J.F. Wang, C.B. Ponton, I.R. Harris, IEEE Trans. Magn. 38 (2002) 2928-2930.
6. J.F. Wang, C.B. Ponton, I.R. Harris, J. Magn. Magn. Mater. 298 (2006) 122-131.
7. K.K. Mallick, P. Shepherd, R.J. Green, J. Magn. Magn. Mater. 312 (2007) 418-429.
8. P.A. Mariño-Castellanos, A.C. Moreno-Borges, G. Orozco-Melgar, J.A. García, E. Govea-Alcaide, Physica B 406 (2011) 3130-3136.
9. M.Q. Liu, X.Q. Shen, F.Z. Song, J. Xiang, X.F. Meng, J. Solid State Chem.184 (2011) 871-876.
10. S. Ounnunkad, P. Winotai, J. Magn. Magn. Mater. 301 (2006) 292-300.
11. P.A. Mariño-Castellanos, J.C. Somarriba-Jarque, J. Anglada-Rivera, Physica B 362 (2005) 95-102.
12. Y.J. Yang, X.S. Liu, D.L. Jin, Y.Q. Ma, Mater. Res. Bull. 59 (2014) 37-41.
13. X.X. Liu, J.M. Bai, F.L. Wei, Z. Yang, J. Appl. Phys. 87 (2000) 6875-6877.
14. L. Qiao, L.S. You, J.W. Zheng, L.Q. Jiang, J.W. Sheng, J. Magn. Magn. Mater. 318 (2007) 74-78.
15. Y.J. Yang, X.S. Liu, Mater. Tech. 29 (2014) 232-236.
16. ([15]) C. Singh, S. Bindra Narang, I.S. Hudiara, Y. Bai, K. Marina, Mater. Lett. 63 (2009) 1921-1924.
17. Y.J. Yang, F.H. Wang, J.X. Shao, D.H. Huang, Z.H. Gao, Q.L. Cao, M.J. Wan, J. Mater. Res. 30 (2015) 1844-1851.
18. D.M. Hemeda, O.M. Hemeda, J. Magn. Magn. Mater. 320 (2008)1557-1562.

19. 1X.S. Liu, W. Zhong, S. Yang, Z. Yu, B.X. Gu, Y.W. Dou, Phys. Stat. Sol. A 193 (2002) 314-319.
20. Y.P. Wang, L.C. Li, H. Liu, H.Z. qiu, F. Xu, Mater. Lett. 62 (2008) 2060-2062.
21. F. Kools, A. morel, R. Grössinger, J.M. Le Breton, P. Tenaud, J. Magn. Magn. Mater. 242-245 (2002) 1270-1276.
22. C.J. Li, B. Wang, J.N. Wang, J. Magn. Magn. Mater. 324 (2012) 1305-1311.
23. S.Qunnunkad, Solid State Commun. 138 (2006) 472-475.
24. A. Thakur, R.R. Singh, P.B. Barman, J. Magn. Magn. Mater. 326 (2013) 35-40.